

## Supporting Information

# Single Molecule Magnet Behavior in Heterometallic Decanuclear $[Ln_2Fe_8]$ ( $Ln=Y, Dy, Ho, Tb, Gd$ ) Coordination Clusters

Man-Ting Chen, Hai-Xia Zhao,\* La-Sheng Long\* and Lan-Sun Zheng

Collaborative Innovation Center of Chemistry for Energy Materials, State Key Laboratory of Physical Chemistry of Solid Surfaces and Department of Chemistry, College of Chemistry and Chemical Engineering, Xiamen University, Xiamen, 361005, China.

## X-ray crystallography

The SQUEEZE<sup>1</sup> analyses show that there are  $656 \text{ \AA}^3$  voids and 164 electron counts per unit cell for **1**, and  $627 \text{ \AA}^3$  voids and 124 electron counts per unit cell for **2**, and  $586 \text{ \AA}^3$  voids and 106 electron counts per unit cell for **3**, and  $738 \text{ \AA}^3$  voids and 125 electron counts per unit cell for **4**, and  $680 \text{ \AA}^3$  voids and 138 electron counts per unit cell for **5**. According to the calculation, there should be extra 8 guest water molecules per formula unit for **1**, and 6 guest water molecules for **2**, and 5 guest water molecules for **3**, and 6 guest water molecules for **4** and 7 guest water molecules for **5** based on the calculation. The counter anions and guest water molecules for the **1–5** were further determined by combining them with the charge balance and the results of EA and TGA. The results showed that there were 6  $\text{ClO}_4^-$  counter anions and 8 guest water molecules in **1**, 6  $\text{ClO}_4^-$  and 6 guest water molecules in **2**, 6  $\text{ClO}_4^-$  and 6 guest water molecules in **3**, 6  $\text{ClO}_4^-$  and 7 guest water molecules in **4**, 6  $\text{ClO}_4^-$  and 7 guest water molecules in **5**. Crystallographic data were summarized in Table S1. CCDC No. 2195974–2195975 for **1–2** and 2314827–2314829 for **3–5**. The data can be obtained free of charge from the Cambridge Crystallographic Data Centre.

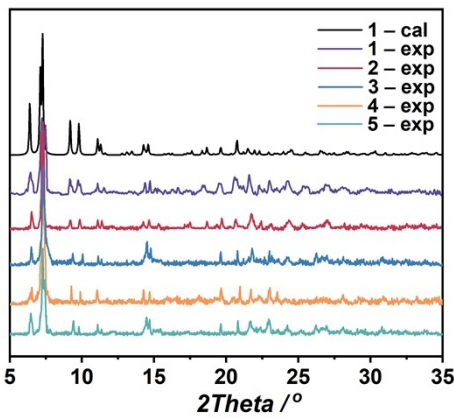


**Figure S1.** Powder X-ray diffraction (XRD) patterns for **1–5**.

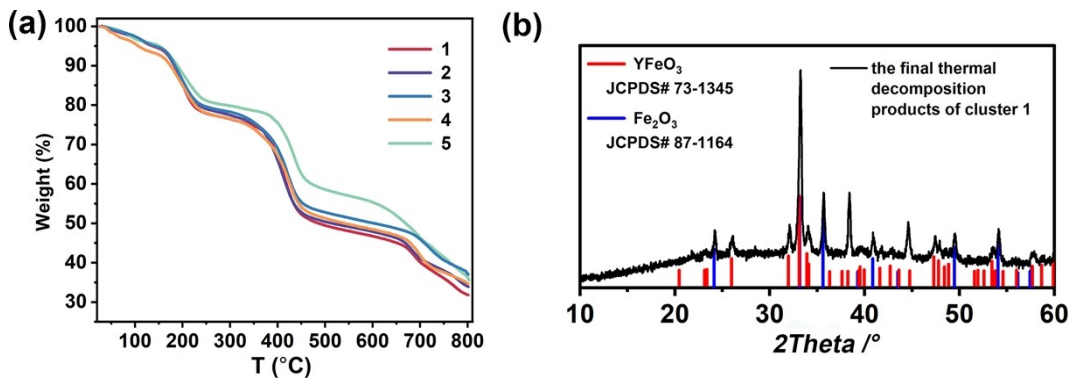


**Figure S2.** (a) The TGA measurement of **1 – 5** under  $\text{N}_2$  atmosphere. (b) XRD for the final thermal decomposition product of **1**.

As shown in Figure S2a, the TGA found that the mass losses of cluster **1** was about 5.19 % at 140°C, which was close to the calculated values of 5.29 % for the removal of 8 guest water molecules. The XRD confirmed that the final thermal decomposition product of **1** was a mixed phase, mainly including  $\text{YFeO}_3$  and  $\text{Fe}_2\text{O}_3$  (Figure S2b). Clusters **2 – 5** display mass losses of approximately 3.81 %, 3.95 %, 5.58 % and 4.03 % about 120°C, which were close to the calculated values of 3.87 %, 3.81 %, 4.43 % and 4.44 % for the removal of guest water molecules, respectively. As the temperature increased, the metal frameworks drastically collapsed.

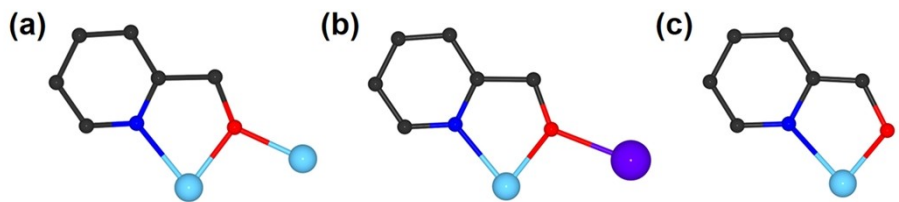


**Figure S3.** The coordination modes of  $\text{hmp}^-$  in **1**. Purple Y; sky blue Fe; red O; dark blue N; and dark gray C.

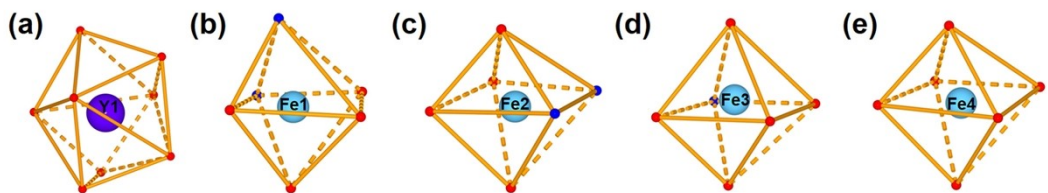


**Figure S4.** The coordination geometries of Y and Fe atoms in **1**. Purple Ln; sky blue Fe; red O; dark blue N.

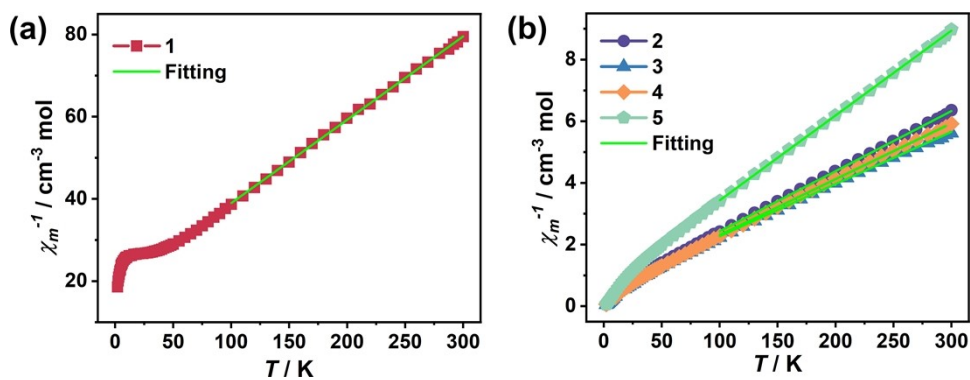


**Figure S5.** The fitting of  $\chi_m^{-1}$  vs  $T$  based on Curie-Weiss law above 100 K for **1–5**.

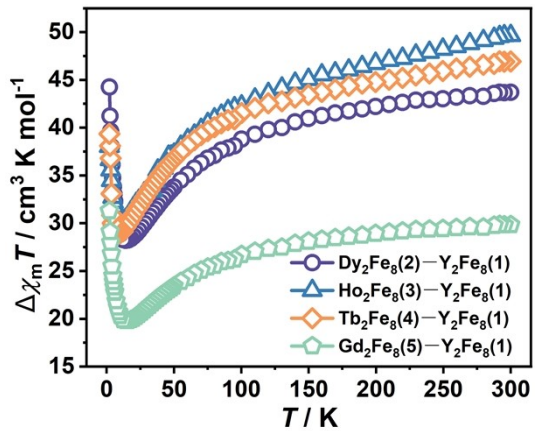


**Figure S6.** The plots of  $\Delta\chi_m T$  versus  $T$  for **1–5**.

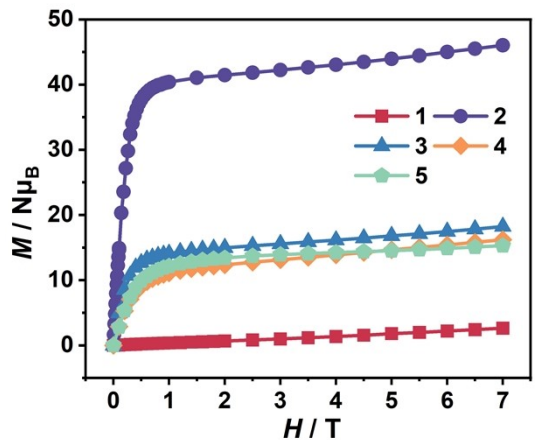


**Figure S7.** Magnetization versus  $H/T$  for **1–5**.

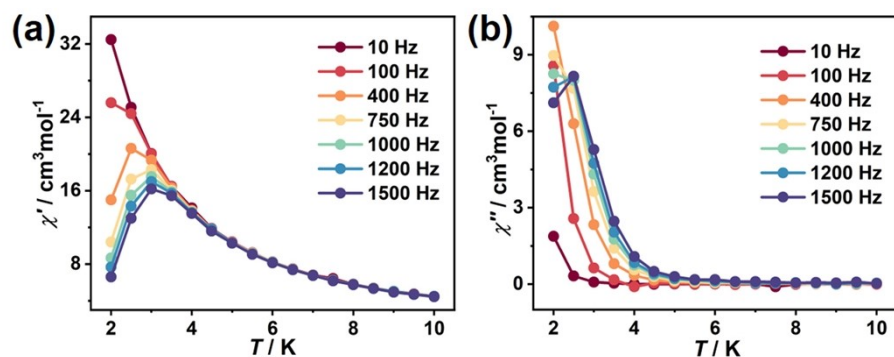


**Figure S8.** (a) Temperature dependence of the in-phase and (b) out-of-phase *ac* susceptibility for **2** under zero *dc* field.

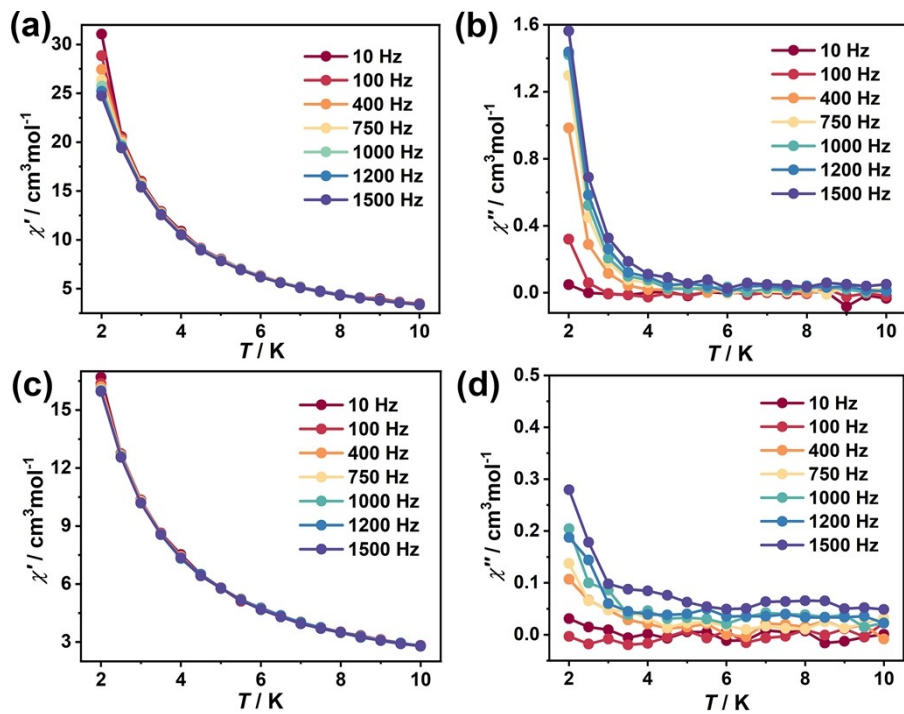


**Figure S9.** Temperature dependence of the in-phase and out-of-phase *ac* susceptibility for **3** (a-b) and **4** (c-d) under zero *dc* field.

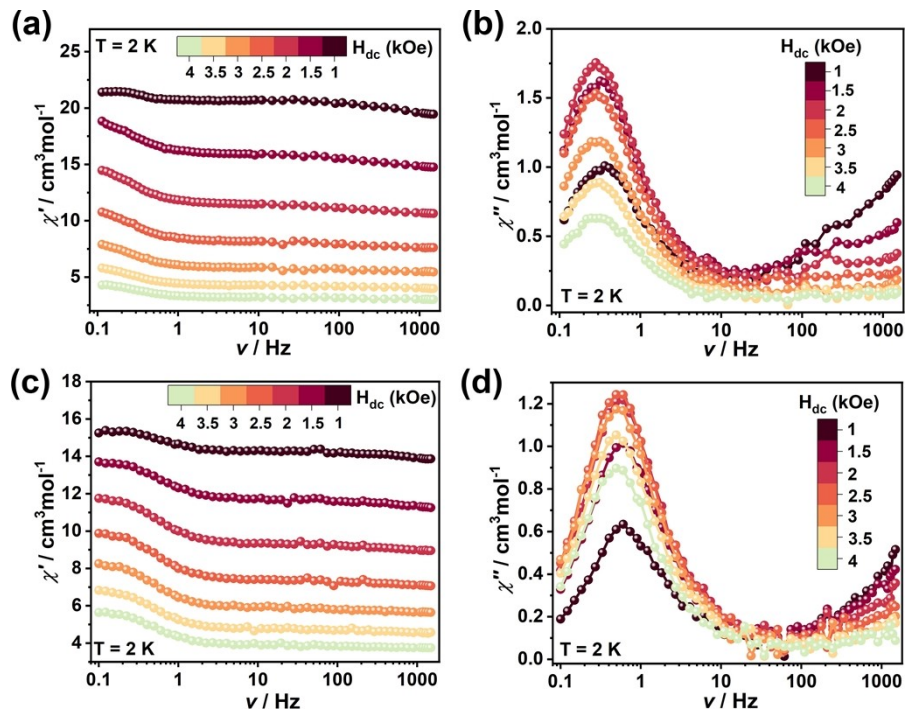


**Figure S10.** Frequency dependence of in-phase and out-of-phase *ac* susceptibility data under different *dc* fields at 2 K for **3** (a-b) and **4** (c-d).

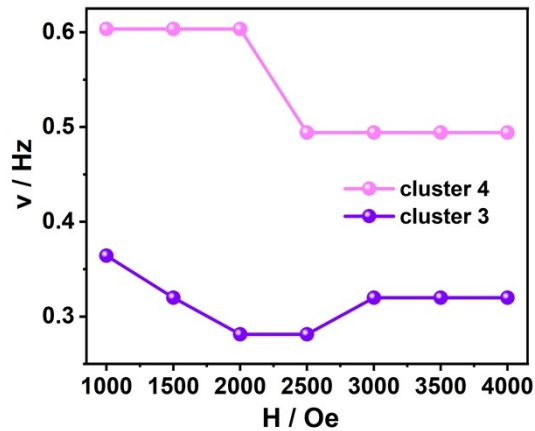


**Figure S11.** Plots of the frequency corresponding to the peak of the out-of-phase susceptibilities vs. applied *dc* magnetic fields at 2 K for **3** and **4**.

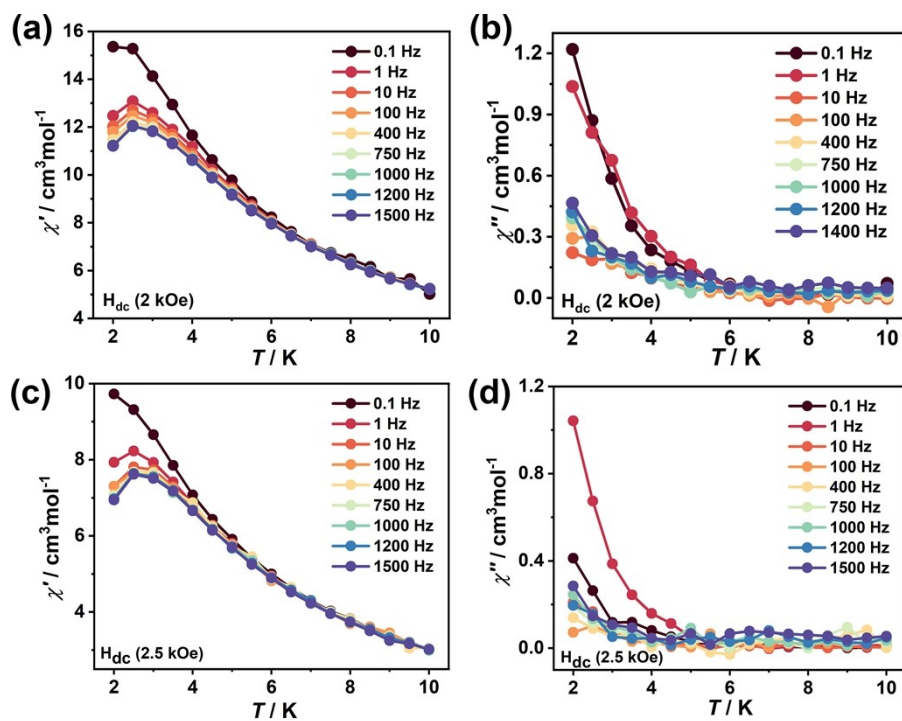


**Figure S12.** (a) Temperature dependence of the in-phase and (b) out-of-phase *ac* susceptibility for **3** under 2 kOe *dc* field. (c) Temperature dependence of the in-phase and (d) out-of-phase *ac* susceptibility for **4** under 2.5 kOe *dc* field.

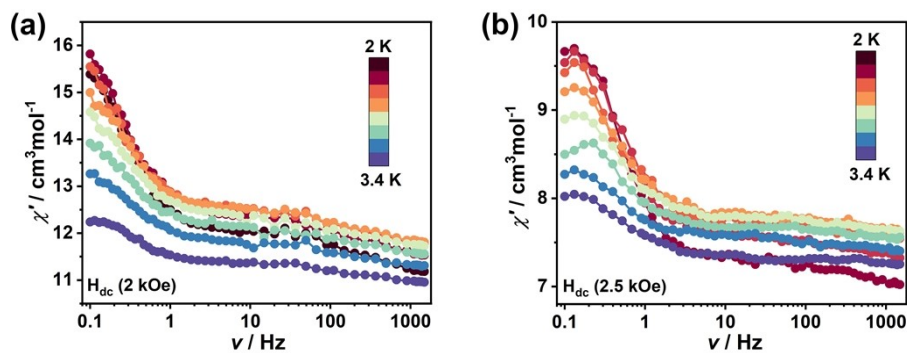


**Figure S13.** The frequency dependence of the  $\chi'$  signals for (a) **3** under 2 kOe, (b) for **4** under 2.5 kOe optimum external magnetic field.

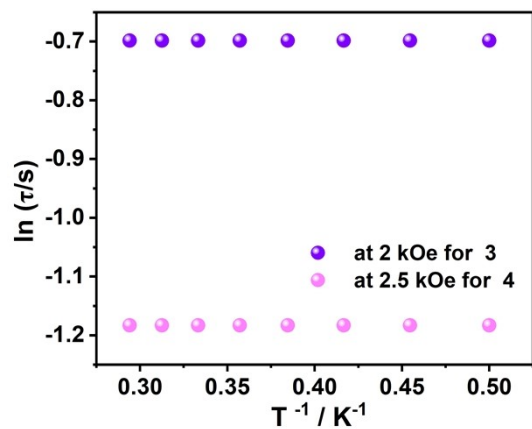


**Figure S14.** The curves of  $\ln \tau$  vs  $T^{-1}$  plots for **3** and **4** under optimal 2 kOe and 2.5 kOe *dc* fields, respectively.

**Table S1** Single Crystal X-ray Structure Refinement of **1–5**.

Compound	<b>1</b>	<b>2</b>	<b>3</b>	<b>4</b>	<b>5</b>
Temperature/K	100	100	100	100	100
Crystal system	Monoclinic	Monoclinic	Monoclinic	Monoclinic	Monoclinic
Space group	<i>P</i> 2 <sub>1</sub> / <i>n</i>				
<i>a</i> / Å	13.7425(3)	13.6830(4)	13.7852(2)	13.6194(4)	13.8630(3)
<i>b</i> / Å	13.5084(2)	13.4980(3)	13.5126(2)	13.4851(3)	13.5261(3)
<i>c</i> / Å	27.6067(4)	27.6595(5)	27.5746(3)	27.7249(5)	27.5985(4)
$\alpha$ / °	90	90	90	90	90
$\beta$ / °	91.845(2)	91.624(2)	91.730(1)	91.360(2)	91.729(2)
$\gamma$ / °	90	90	90	90	90
<i>V</i> / Å <sup>3</sup>	5122.23(15)	5106.5(2)	5134.09(12)	5090.5(2)	5172.70(18)
<i>Z</i>	2	2	2	2	2
<i>D</i> <sub>c</sub> / g cm <sup>-3</sup>	1.680	1.781	1.786	1.762	1.744
Reflections collected	34779	31379	33887	31963	21290
<i>F</i> (000)	2608.0	2716.0	2724.0	2680.0	2686.0
GOOF	1.017	1.031	1.057	1.055	1.040
<i>R</i> <sub>1</sub> [ <i>I</i> > 2σ( <i>I</i> )]	0.0701	0.0701	0.0643	0.0816	0.0875
<i>wR</i> <sub>2</sub> [ <i>I</i> > 2σ( <i>I</i> )]	0.1879	0.1942	0.1942	0.2179	0.2410
<i>R</i> <sub>1</sub> (All data)	0.0942	0.0908	0.0747	0.1073	0.0999
<i>wR</i> <sub>2</sub> (All data)	0.2089	0.2118	0.2052	0.2413	0.2629

$$R_1 = \sum |F_O| - |F_C| / \sum |F_O|, wR_2 = \{\sum [w(F_O^2 - F_C^2)^2] / \sum [w(F_O^2)^2]\}^{1/2}$$

**Table S2.** Bond Valence Sum calculations for Fe atoms of **1–5**.

Atom	<b>1</b>	<b>2</b>	<b>3</b>	<b>4</b>	<b>5</b>
	BVS	BVS	BVS	BVS	BVS
Fe1	3.016	3.035	3.063	3.058	3.044
Fe2	3.008	2.956	2.983	3.001	2.993
Fe3	2.997	2.992	2.983	3.027	2.939
Fe4	2.933	2.963	3.031	3.057	2.979

**Table S3.** Cole-Cole curve fitting parameters of **2**.

Temperature(K)	$\tau$	$\alpha$	$X_T$	$X_S$
2	5.71965E-4	0.29114	23.16464	0.72423
2.2	2.65488E-4	0.26055	20.2307	0.86813
2.4	1.59155E-4	0.26112	18.68795	0.92554
2.6	7.38743E-5	0.25174	17.49265	1.04649
2.8	4.4286E-5	0.24005	15.98472	1.20259
3	2.65488E-5	0.21681	14.6561	1.65402
3.2	2.05557E-5	0.19086	13.66059	2.2433
3.4	1.59155E-5	0.15561	12.35776	2.4019

**Table S4.** Selected bond distances ( $\text{\AA}$ ) and bond angles ( $^{\circ}$ ) of **1**.

Bond	Dis( $\text{\AA}$ )	Bond	Angel( $^{\circ}$ )
Y1–O1	2.493(4)	O12–Y1–O20	77.17(17)
Y1–O4 <sup>1</sup>	2.373(5)	O1–Y1–O4 <sup>1</sup>	68.64(16)
Y1–O12	2.279(5)	O18–Y1–O13	78.9(2)
Fe1–O10	1.976(5)	O13–Y1–O1	123.21(19)
Fe1–O12	1.950(5)	O1–Fe1–O12	86.0(2)
Fe2–O14 <sup>1</sup>	1.980(5)	O1–Fe1–N1	97.6(2)
Fe2–O24	2.008(6)	O32–Fe2–N5	91.2(3)
Fe3–O24	2.071(5)	O4–Fe3–O12	97.5(2)
Fe4–O1 <sup>1</sup>	2.031(5)	O22–Fe3–O10	96.5(2)
Fe4–O14	1.964(5)	O31–Fe4–O6A <sup>1</sup>	99.1(3)

<sup>1</sup>1-X,1-Y,1-Z

**Table S5.** Selected bond distances ( $\text{\AA}$ ) and bond angles ( $^{\circ}$ ) of **2**.

Bond	Dis( $\text{\AA}$ )	Bond	Angel( $^{\circ}$ )
Dy1–O1	2.504(4)	O6–Dy1–O37	84.81(19)
Dy1–O4 <sup>1</sup>	2.371(5)	O37–Dy1–O4 <sup>1</sup>	68.29(18)
Dy1–O6	2.297(5)	O6–Dy1–O22	77.10(17)
Fe1–O1	1.917(5)	O37–Dy1–O1	85.87(16)
Fe1–O12	1.979(5)	O1–Fe1–O6	86.5(2)
Fe2–O8	1.981(5)	O6–Fe1–N1	107.1(2)
Fe2–O26	2.024(6)	O8–Fe2–N3	163.5(3)
Fe3–O4	1.956(5)	O4–Fe3–O12	97.5(2)
Fe4–O1 <sup>1</sup>	2.044(4)	O12–Fe3–O26 <sup>1</sup>	164.4(2)
Fe4–O8	1.963(5)	O38–Fe4–O4 <sup>1</sup>	171.3(2)

<sup>1</sup>1-X,1-Y,1-Z**Table S6.** Selected bond distances ( $\text{\AA}$ ) and bond angles ( $^{\circ}$ ) of **3**.

Bond	Dis( $\text{\AA}$ )	Bond	Angel( $^{\circ}$ )
Ho1–O1	2.283(4)	O6–Ho1–O7	68.30(13)
Ho1–O4 <sup>1</sup>	2.307(4)	O1–Ho1–O4 <sup>1</sup>	97.06(15)
Ho1–O8	2.424(5)	O1–Ho1–O8	82.96(17)
Fe1–O3	1.983(4)	O10–Ho1–O6	68.42(14)
Fe1–O2	2.076(4)	O7–Fe1–O1	86.27(17)
Fe2–O7	1.952(4)	O1–Fe1–N1	77.78(19)
Fe2–O6	2.067(4)	O7–Fe2–O5	103.75(17)
Fe3–O10	1.925(5)	O6–Fe3–O12	82.46(18)
Fe4–O3 <sup>1</sup>	2.012(4)	O3 <sup>1</sup> –Fe4–O2 <sup>1</sup>	75.81(16)
Fe4–O14	1.905(11)	O14–Fe4–O3 <sup>1</sup>	92.4(8)

<sup>1</sup>1-X,1-Y,1-Z

**Table S7.** Selected bond distances ( $\text{\AA}$ ) and bond angles ( $^{\circ}$ ) of **4**.

Bond	Dis( $\text{\AA}$ )	Bond	Angel( $^{\circ}$ )
Tb1–O1	2.278(6)	O9–Tb1–O6	128.1(3)
Tb1–O11 <sup>1</sup>	2.313(6)	O1–Tb1–O11 <sup>1</sup>	96.8(2)
Tb1–O5	2.421(8)	O8–Tb1–O5	139.2(3)
Fe1–O3	2.070(6)	O7–Tb1–O4	140.3(2)
Fe1–O2	1.983(6)	O2–Fe1–O3	77.0(3)
Fe2–O9	1.990(7)	O1–Fe1–N3	107.5(3)
Fe2–O12	2.013(8)	O9–Fe2–N4	111.3(3)
Fe3–O9	2.065(6)	O11–Fe3–O9	171.4(3)
Fe4–O2 <sup>1</sup>	2.000(7)	O4 <sup>1</sup> –Fe3–O3 <sup>1</sup>	78.0(2)
Fe4–O13	1.885(8)	O12–Fe4–O3 <sup>1</sup>	89.3(3)

<sup>1</sup>1-X,1-Y,1-Z**Table S8.** Selected bond distances ( $\text{\AA}$ ) and bond angles ( $^{\circ}$ ) of **5**.

Bond	Dis( $\text{\AA}$ )	Bond	Angel( $^{\circ}$ )
Gd1–O6	2.384(7)	O9–Gd1–O6	153.2(2)
Gd1–O1 <sup>1</sup>	2.358(6)	O1 <sup>1</sup> –Gd1–O7	87.0(2)
Gd1–O14	2.452(6)	O7–Gd1–O13	144.6(2)
Fe1–O9	1.956(6)	O13–Gd1–O14	66.8(2)
Fe1–O3	1.913(5)	O3–Fe1–O9	87.0(2)
Fe2–O2	2.17(5)	O3–Fe1–N6	164.2(3)
Fe2–O7	2.052(6)	O1–Fe2–O4	99.1(16)
Fe3–O12	1.892(8)	O12–Fe3–O7	98.7(3)
Fe4–O8	1.937(7)	O5–Fe4–O11	93.0(3)
Fe4–O11	2.011(7)	O8–Fe4–O5	101.7(3)

<sup>1</sup>1-X,1-Y,1-Z

## Reference

- (1) Spek, A. L. PLATON SQUEEZE: A Tool for the Calculation of the Disordered Solvent Contribution to the Calculated Structure Factors. *Acta. Crystallogr. Sect. C Struct. Chem.* **2015**, *71*, 9–18.